sustainability

MDPI

Article

Effects of Silicic Acid on Leaching Behavior of Arsenic from Spent Magnesium-Based Adsorbents Containing Arsenite

Hajime Sugita *, Terumi Oguma, Junko Hara, Ming Zhang and Yoshishige Kawabe

Geological Survey of Japan, National Institute of Advanced Industrial Science and Technology (AIST), Central 7, 1-1-1 Higashi, Tsukuba 305-8567, Japan; t.oguma@aist.go.jp (T.O.); j.hara@aist.go.jp (J.H.); m.zhang@aist.go.jp (M.Z.); y-kawabe@aist.go.jp (Y.K.)

* Correspondence: hajime.sugita@aist.go.jp

Abstract: The spent adsorbents left after treating arsenic-contaminated water contain large amounts of arsenic. These spent adsorbents may come into contact with silicic acid leached from soil or cementitious solidification materials in the disposal environment. Thus, it is important to evaluate the effects of silicic acid on spent adsorbents containing arsenic. In this study, the effects of silicic acid on spent Mg-based adsorbents (magnesium oxide (MgO) and magnesium hydroxide ($Mg(OH)_2$)) containing arsenite were investigated. The arsenic leaching ratios of both spent adsorbents decreased slightly with an increase in the initial silicic acid concentration of the eluent. The arsenic leaching ratio decreased from 1.24% to 0.69% for MgO and from 5.97% to 4.71% for $Mg(OH)_2$ at an initial Si-normalized concentration of 100 mg/L. The primary mechanism behind the inhibition of arsenic leaching by silicic acid was determined to be the difficulty of arsenic desorption due to the coating effect following the adsorption of silicic acid species. The results indicate that the arsenic leaching related to the ion exchange reaction with silicic acid hardly occurred for the spent Mg-based adsorbents. Compared with various spent Mg-based and Ca-based adsorbents, the spent MgO adsorbent exhibited the highest environmental stability and best performance.

Keywords: disposal; environmental stability; leaching ratio; ion exchange reaction; hydroxide ion

check for updates

Citation: Sugita, H.; Oguma, T.; Hara, J.; Zhang, M.; Kawabe, Y. Effects of Silicic Acid on Leaching Behavior of Arsenic from Spent Magnesium-Based Adsorbents Containing Arsenite. *Sustainability* **2022**, *14*, 4236. https://doi.org/10.3390/su14074236

Academic Editors: Ken Kawamoto, Tomonori Ishigaki and Hoang Giang Nguyen

Received: 9 March 2022
Accepted: 28 March 2022
Published: 2 April 2022

Publisher's Note: MDPI stays neutral with regard to jurisdictional claims in published maps and institutional affiliations.

Copyright: © 2022 by the authors. Licensee MDPI, Basel, Switzerland. This article is an open access article distributed under the terms and conditions of the Creative Commons Attribution (CC BY) license (https://creativecommons.org/licenses/by/4.0/).

1. Introduction

The arsenic (As) pollution of groundwater occurs in many regions of the world and is a major global problem [1,2]. The guidelines of the World Health Organization (WHO) for drinking water quality include a provisional guideline value for As (0.01 mg/L) and some notable points about its properties and health effects [3]. For instance, the guidelines note that the most important routes of As exposure are via the consumption of food and drinking water, including beverages that are made from drinking water. Signs of chronic arsenicism, including dermal lesions (e.g., hyperpigmentation and hypopigmentation), peripheral neuropathy, skin cancer, bladder and lung cancers, and peripheral vascular disease, have been observed in populations ingesting As-contaminated drinking water [3]. There is overwhelming evidence that the consumption of drinking water containing elevated As concentrations is causally related to the development of cancer. In addition, acute As intoxication associated with the ingestion of well water containing very high As concentrations (21 mg/L) has been reported [3]. In view of the practical difficulties in removing As from drinking water, particularly from small supplies, and the practical quantification limit for As, the provisional guideline value of 0.01 mg/L is retained as a goal.

It is essential to treat As-contaminated water to prevent the health damage caused by As. In developing countries, treatment methods involving inexpensive adsorbents are more likely to be used owing to economic and operational conditions. However, it is also important to prioritize the convenience and environmental friendliness of treatment

methods in order to realize a sustainable society. The spent adsorbents remaining after treating As-contaminated water contain large amounts of As, and may come into contact with silicic acid leached from soil or cementitious solidification materials in the disposal environment. Silicic acid (silica) is a major component of soil and rocks, and is abundant in the environment. The chemistry of silicic acid (solubility, polymerization rate, etc.) is so interesting that it has been studied by many researchers for a long time [4–11]. However, the effects of silicic acid on adsorbents in the waste environment have not yet been investigated. Thus, it is important to evaluate the effects of silicic acid on spent adsorbents. Previous studies have examined the effects of silicic acid on the environmental stabilities of spent calcium (Ca)-based adsorbents containing arsenate (As(V)) and arsenite (As(III)) [12,13].

Currently, magnesium (Mg)-based adsorbents such as MgO and $Mg(OH)_2$ are expected to be used as adsorbents for CO_2 recovery for the purpose of preventing global warming [14–17], in addition to removing various heavy metals and organic compounds [18–25]. Mg is a safe substance in terms of human health. Similar to Ca-based adsorbents (i.e., Ca as the base material) [26–29], Mg-based adsorbents are also environmentally friendly, and many researchers have studied As removal using Mg-based adsorbents [30–33]. For example, Park et al. [30] investigated adsorption on magnesium hydroxide ($Mg(OH)_2$) and the precipitation of $Mg_3(AsO_4)_2$ for As(V) removal from a molybdenum oxide processing plant liquor. The addition of magnesium oxide (MgO) as a precipitating agent was also tested. The authors modeled the speciation and solubility equilibria using software, and identified the pH conditions at which optimum precipitation could be carried out. Magnesium solutions made by dissolving $MgSO_4$ or $MgCl_2$ in distilled water were then added to the liquor at Mg:As molar ratios of between 1:1 and 4:1, and $Mg(OH)_2$ started to precipitate at a solution pH of more than 9.3. As their model predicted that no $Mg_3(AsO_4)_2$ could be formed at a pH value of more than 11, the authors considered that the removal of As(V) at such pH values was mainly due to its adsorption onto $Mg(OH)_2$. However, the actual amount of As(V) removed exceeded the predicted value, due to the precipitation of $Mg_3(AsO_4)_2$ and the adsorption of As(V) to $Mg(OH)_2$, which precipitates in the pH range of 10–11. Although $MgCl_2$ and $MgSO_4$ were both equally effective precipitating agents for As(V) removal when added to the stripped liquors at pH 10.3, MgO was not effective. In another study, Tresintsi et al. [31] proposed a procedure based on granulated MgO to regenerate spent iron oxy-hydroxide adsorbents used for As removal. Iron oxy-hydroxides are the most widely used class of As adsorbents because they can remove both As(III) and As(V). Although iron oxy-hydroxide adsorbents are expensive, regenerating them could significantly reduce the total cost of water treatment [31]. As a low-cost material that is easy to manufacture from abundant natural minerals, Tresintsi et al. performed both batch adsorption tests and column tests using MgO to recover arsenic desorbed from the iron oxy-hydroxide adsorbent [31]. In the column tests, only As(V) was investigated, because the removal efficiency of As(III) is much lower than that of As(V), and As(III) would have converted into As(V) in the actual pretreatment stage. In the column test, a sodium hydroxide (NaOH) solution was first fed through a column filled with a spent iron oxy-hydroxide adsorbent to desorb As, and was then continuously fed through another column filled with MgO. The regeneration process was completed in 24 h, and the regeneration of the adsorbent confirmed that the initial removal efficiency was restored by approximately 80%. The X-ray absorption near edge structure (XANES) spectra of As adsorbed on MgO obtained in the batch tests confirmed that As(III) was not oxidized to As(V) during the adsorption process. The authors proposed that the mechanism of As adsorption onto MgO involves hydrolysis, while the mechanism of As(V) adsorption onto $Mg(OH)_2$ involves chemisorption. Finally, based on the results of their leaching and mechanical strength tests, the authors concluded that spent MgO could be used as an additive in building materials.

Although adsorption treatment has been widely used to remove As from water, owing to its simplicity and cost effectiveness, some pretreatment processes, such as the oxidation of As(III) to As(V) and the adjustment of the pH value, lead to higher running costs and more complex operations [32]. Therefore, Yu et al. [32] aimed to develop a hierarchically

micro/nanostructured MgO adsorbent that could effectively remove both As(III) and As(V). First, two MgO precursors were prepared from $Mg(NO)_3$ and K_2CO_3 solutions. The MgO precursors were confirmed to be hydromagnesites ($MgCO_3$ hydrates) by X-ray diffraction (XRD). The hydromagnesites did not have a high removal performance for As; however, MgO nanoflakes prepared by calcining the hydromagnesites had a high removal performance for both As(III) and As(V). The authors concluded that the entire adsorption procedure involved the reaction of partial MgO with water to form $Mg(OH)_2$, the adsorption of As onto MgO and $Mg(OH)_2$, and the reaction between As and $Mg(OH)_2$. Opiso et al. [33] investigated the different mineral phases formed under alkaline conditions in a Mg–Si–Al system, and the sorption behavior of As(V) during and after mineral formation. They conducted coprecipitation experiments, adsorption experiments, and desorption experiments on As(V). The synthesis in the Mg–Si–Al system at 25 °C resulted in the formation of brucite ($Mg(OH)_2$), hydrotalcite ($Mg_6Al_2(CO_3)(OH)_{16}{\cdot}4(H_2O)$), and poorly crystalline serpentine-like materials ($MgSi_2O_5(OH)_4$). Brucite formation occurred in the high Mg content system in the absence of Al. By comparing the As removal efficiencies of the minerals formed during the co-precipitation experiments at 25 °C, it was found that the removal efficiency of As(V) increased as the Mg content increased, whereas it decreased as the Al content increased. In the co-precipitation experiments at 50 °C, the amount of arsenate co-precipitated by brucite was higher than that co-precipitated by amorphous magnesium silicate. The amount of adsorbed As(V) in the adsorption experiments was lower than that in the co-precipitation experiments. The higher removal efficiency of As(V) during mineral formation suggests that, in addition to surface adsorption, As(V) incorporation is also a dominant mechanism. Moreover, the As removal efficiencies of minerals during the adsorption experiments were not influenced by the Mg concentration in the solution. The results show that brucite, hydrotalcite ($Mg_6Al_2(CO_3)(OH)_{16}{\cdot}4(H_2O)$) and serpentine ($MgSi_2O_5(OH)_4$) had high uptake capacities for As(V). However, As incorporation was only observed during the formation of high-Al content hydrotalcite and serpentine minerals, and was greatly enhanced at higher temperatures. In addition, the results of X-ray absorption fine structure (XAFS) analyses indicate that the co-precipitated As mainly existed in its pentavalent form.

Similar to spent Ca-based adsorbents, spent Mg-based adsorbents that have adsorbed As ultimately also become waste materials containing large amount of As. Our previous study [34] examined the effects of silicic acid on the environmental stability of Mg-based adsorbents (MgO, $Mg(OH)_2$, and $MgCO_3$) containing As(V). The results show that the spent adsorbents based on $Mg(OH)_2$ and $MgCO_3$ were strongly affected by silicic acid, which significantly increased As leaching and also reduced their environmental stabilities. In contrast, As leaching from the spent MgO-based adsorbent was very low, and the environmental stability of the adsorbent was extremely high. However, this study focused on As(V), and no similar tests have been conducted on As(III). As mentioned in the WHO's guidelines [3], As is often reduced to As(III) underground, and As(III) is widely known to be more toxic than As(V). Understanding the leaching behavior of arsenous acid is very important. Accordingly, the present study investigated two spent Mg-based adsorbents (MgO and $Mg(OH)_2$) containing As(III) by performing shaking tests with silicic acid. In these tests, the leaching behaviors of As and Mg from the spent adsorbents, and reductions in the silicic acid concentration of the liquid phase, were investigated. Then, the effects of silicic acid on the environmental stability of each Mg-based adsorbent were evaluated. Finally, a more environmentally friendly adsorbent is recommended by comparing the environmental stability data of spent Mg-based and Ca-based adsorbents obtained in various studies on the effects of silicic acid.

2. Materials and Methods

Unless otherwise specified, the reagents used in this study were purchased from FUJIFILM Wako Pure Chemical Corporation, Osaka, Japan (formerly Wako Pure Chemical Industries, Ltd.).

2.1. Spent Mg-Based Adsorbents

In our previous study on spent Mg-based adsorbents containing As(V) [34], $MgCO_3$, MgO and $Mg(OH)_2$ were investigated. However, our preliminary experiments demonstrated that the arsenite removal performance of $MgCO_3$ was significantly inferior to that of the other two Mg-based adsorbents. In addition, Yu et al. [32] also reported that the As adsorption performance of $MgCO_3$ hydrate was significantly inferior to that of MgO. Therefore, as $MgCO_3$ is not recommended for use alone in arsenite removal treatment, only MgO and $Mg(OH)_2$ were evaluated in this study. The spent Mg-based adsorbents containing As(III) used in the experiments were the same as those used in our previous study [35]. An overview of the preparation of the spent adsorbents is provided below.

2.1.1. Mg-Based Adsorbents (Unspent)

Two types of Mg compound reagents, MgO and $Mg(OH)_2$, were used in this study. These were commercially available and purchased from FUJI-FILM Wako Pure Chemical Co. The nominal purity values of MgO and $Mg(OH)_2$ were 98.0% and 99.9%, respectively. The measured Mg content, median particle size, and Brunauer–Emmett–Teller (BET) surface area of MgO were 59.1%, 1.54 μm, and 4.3 m^2/g, respectively, while those of $Mg(OH)_2$ were 40.6%, 4.13 μm, and 22 m^2/g, respectively [36].

2.1.2. Synthetic As-Contaminated Water

Powdered reagents of sodium arsenite ($NaAsO_2$, 90%) and sodium hydrogen arsenate heptahydrate ($Na_2HAsO_4{\cdot}7H_2O$, 99%) were dissolved in deionized water, and stock solutions of As(III) and As(V) (2000 mg-As/L) were prepared. A portion of each stock solution was diluted with deionized water to prepare a 20 mg-As/L solution. This solution was used as synthetic As-contaminated water after adjusting the pH to near neutral by adding hydrochloric acid (HCl).

2.1.3. Preparation of Spent Mg-Based Adsorbents

One gram of each unspent Mg-based-adsorbent was weighed into a TPX beaker. Synthetic As-contaminated water (200 mL) was added to the beaker and stirred with a magnetic stirrer (approximately 500 rpm). After stirring for approximately 24 h, suction filtration was performed using a Teflon filter (pore size: 0.45 μm) for solid–liquid separation. The concentrations of As and Mg in each filtrate were determined using inductively coupled plasma–mass spectrometry (ICP–MS) (Agilent 7700X or Shimadzu ICPM-8500) and ICP–atomic emission spectrometry (AES) (SII SPS3500DD), respectively. The calculation methods used to determine data pertaining to each filtrate are outlined below [35,36].

Tables 1 and 2 list As and Mg data, respectively, in relation to the production of four types of spent adsorbents containing As(III) or As(V). In Table 1, W_{AD} (g) is the amount of unspent adsorbent added to the synthetic As-contaminated water, and V is the liquid volume (L) of the synthetic As-contaminated water; hence, W_{AD}/V is the amount of unspent adsorbent added per unit volume of As-contaminated water (g/L). pH_0 is the pH of the solution immediately before adding the adsorbent, which is referred to as "the initial pH". C_{AS0} is the initial As concentration (mg/L) of the As-contaminated water, C_{AS} is the As concentration of the filtrate, and R_{AS} is the As removal ratio, which was calculated as follows:

$$R_{AS} = (C_{AS0} - C_{AS})/C_{AS0} \times 100. \quad (1)$$

In Table 2, W_{Mg}/V is the amount of Mg contained in unspent adsorbent added per unit volume of As-contaminated water (mg/L), which was calculated using Equation (2):

$$W_{Mg}/V = W_{AD}/V \times 1000 \times \alpha_{Mg}/100 \quad (2)$$

where α_{Mg} is the Mg content of the Mg-based adsorbent.

Table 1. As data relating to the production of spent Mg-based adsorbents.

No.	Adsorbent	As(Valence)	W_{AD}/V (g/L)	pH_0	C_{AS0} (mg/L)	C_{AS} (mg/L)	R_{AS} (%)
(1) [1]	MgO	As(III)	5.004	6.99	21.792	0.149	99.3
(2) [1]	$Mg(OH)_2$	As(III)	5.007	7.10	21.854	1.013	95.4
(3) [2]	MgO	As(V)	5.028	7.14	21.160	0.016	99.9
(4) [2]	$Mg(OH)_2$	As(V)	5.012	7.11	21.065	0.024	99.9

[1] The data of No. (1) and (2) are from Sugita et al. (2020) [35]. [2] The data of No. (3) and (4) are from Sugita et al. (2016) [36].

Table 2. Mg data relating to the production of spent Mg-based adsorbents.

No.	Adsorbent	As(Valence)	α_{Mg} (%)	W_{Mg}/V (mg/L)	C_{Mg} (mg/L)	β_{Mg} (%)
(1) [1]	MgO	As(III)	59.08	2956	6.23	0.21
(2) [1]	$Mg(OH)_2$	As(III)	40.55	2030	7.80	0.38
(3) [2]	MgO	As(V)	59.08	2971	10.37	0.35
(4) [2]	$Mg(OH)_2$	As(V)	40.55	2032	9.51	0.47

[1] The data of No. (1) and (2) are from Sugita et al. (2020) [35]. [2] The data of No. (3) and (4) are from Sugita et al. (2016) [36].

In Table 2, C_{Mg} is the Mg concentration of the filtrate (i.e., the Mg concentration leached from the adsorbent). β_{Mg} is the Mg leaching ratio, which was calculated as follows:

$$\beta_{Mg} = C_{Mg}/(W_{Mg}/V) \times 100 \quad (3)$$

For both MgO and $Mg(OH)_2$, the R_{AS} and β_{Mg} values for As(III) were slightly lower than those for As(V). In addition, the β_{Mg} values of MgO for both As(III) and As(V) were clearly lower than those of $Mg(OH)_2$.

The adsorbents with As recovered by the solid–liquid separation operation were dried at a low temperature (approximately 40 °C) for approximately 12 h in a constant temperature dryer and then stored in a closed polypropylene bottle. The adsorbents containing As were used as "spent adsorbents" in the shaking test, as described in Section 2.3. The method used to calculate the As content of a spent adsorbent is outlined below [35,36].

The residual ratio of adsorbent γ as a percentage was calculated using Equation (4):

$$\gamma = 100 - \beta_{Mg} \quad (4)$$

The amount of As adsorbed per unit mass of the adsorbent remaining as solid δ (mg-As/g) was calculated using Equation (5):

$$\delta = (C_{AS0} - C_{AS})/[(\gamma/100) \times W_{AD}/V] \quad (5)$$

The weighed value of a spent adsorbent was taken as the total value of the adsorbent and As adsorbed onto its surface. Therefore, the As content per unit mass of the recovered spent adsorbent (Q_{AS}, mg-As/g) was determined using Equation (6):

$$Q_{AS} = \delta/(1 + \delta/1000) \quad (6)$$

Table 3 shows Q_{AS} obtained by previous studies [35,36].

Table 3. As content per unit mass of spent adsorbent.

No.	Adsorbent	As(Valence)	Q_{AS} (mg-As/g)
(1) [1]	MgO	As(III)	4.32
(2) [1]	$Mg(OH)_2$	As(III)	4.16
(3) [2]	MgO	As(V)	4.20
(4) [2]	$Mg(OH)_2$	As(V)	4.20

[1] The data of No. (1) and (2) are from Sugita et al. (2020) [35]. [2] The data of No. (3) and (4) are from Sugita et al. (2016) [36].

2.2. Silicic Acid Solution

The silicic acid solutions used in this study were the same as those reported in previous studies [12,13,34]. Therefore, the detailed preparation method can be found in these publications. Briefly, the Si concentrations of the test solvent were 0 mg/L (i.e., deionized water), 5 mg/L, 25 mg/L, 50 mg/L, and 100 mg/L. The test solvent was the silicic acid solution obtained after the pH was neutralized with HCl and NaOH immediately before adding the spent adsorbent in the shaking test (pH_0 = 6.95–7.41) [12]. The total Si concentration was measured using ICP-AES, and the monosilicic acid (silica monomer) concentration was measured using the molybdenum yellow method. Silicic acid refers to H_4SiO_4 (or $Si(OH)_4$), and silica refers to SiO_2. However, in this study, all concentrations of silicic acid species were described as values converted to the Si concentration. Here, the Si concentration is referred to as the "Si-normalized concentration", as in a previous study [12]. The Si-normalized concentrations quantified using ICP-AES and the molybdenum yellow method are referred to as the "total Si-normalized concentration" and "Si-normalized monomer concentration", respectively, and are denoted as $C_{Si\text{-}T}$ and $C_{Si\text{-}M}$. However, as the $C_{Si\text{-}M}$ measurements were approximately equal to those of $C_{Si\text{-}T}$, only $C_{Si\text{-}T}$ was taken as the Si-normalized concentration, as similar to a previous study [12].

2.3. Shaking Test with Spent Mg-Based Adsorbents and Silicic Acid Solution

The procedure used for the shaking tests is described in full elsewhere [12,13,34]. Briefly, approximately 0.1 g of a spent adsorbent (MgO or $Mg(OH)_2$) and 50 mL of the test solvent (either deionized water or the silicic acid solution at each Si concentration) were added to a reaction tube (50 mL polypropylene centrifuge tube). The tube was sealed with a cap and shaken in a thermostatic shaker (150–180 rpm) at room temperature. After shaking for 24 h, the tube was placed in a centrifuge (4500 rpm) for 20 min. After centrifugation, the supernatant was filtered through a syringe filter (0.45 µm pore size), and the filtrate (eluate) was collected in a polypropylene bottle. The As concentration in each eluate was measured using ICP-MS, and the concentrations of Mg and Si were measured using ICP-AES. To confirm their reproducibility, the shaking tests using the spent Mg-based adsorbents were conducted three times under the same conditions ($C_{Si\text{-}T0}$ = 50 mg/L).

3. Results

3.1. pH of Eluate

Table 4 lists the pH_f of each eluate obtained during the shaking tests. The $C_{Si\text{-}T0}$ values in Table 4 are the corresponding values of the Si-normalized concentration. Figure 1 presents a plot of pH_f versus $C_{Si\text{-}T0}$. For comparison with As(III), the results for the spent Mg-based adsorbents containing As(V) (reported in our previous study [34]) are also shown in Table 4 and Figure 1. Although the pH_0 values were near neutral (i.e., 6.95–7.41), the pH increased significantly after adding the spent adsorbents. As shown in Figure 1, the pH_f values of the eluates obtained from MgO containing As(III), and MgO containing As(V), were higher than those obtained from $Mg(OH)_2$ containing As(III) and $Mg(OH)_2$ containing As(V). In addition, no significant difference was observed between the pH_f values of the eluates obtained from $Mg(OH)_2$ containing As(III) and $Mg(OH)_2$ containing As(V). In contrast, at a $C_{Si\text{-}T0}$ value of 100 mg/L, the pH_f values of the eluates obtained from MgO containing As(V) were higher than those obtained from MgO containing As(III),

whereas no significant difference was observed when the $C_{Si\text{-}T0}$ value was between 0 and 50 mg/L.

Table 4. pH values of eluates (pH_f).

	$C_{Si\text{-}T0}$ (mg/L)		0	5	25	50	100
No.	**Adsorbent**	**As(Valence)**			pH_f		
(1)	MgO	As(III)	10.66	10.75	10.74	10.72	10.32
(2)	$Mg(OH)_2$	As(III)	10.49	10.39	10.02	9.74	9.38
(3) [1]	MgO	As(V)	10.79	10.81	10.72	10.83	10.64
(4) [1]	$Mg(OH)_2$	As(V)	10.38	10.26	9.95	9.66	9.47

[1] The values of No. (3) and (4) are from Sugita et al. (2017) [34].

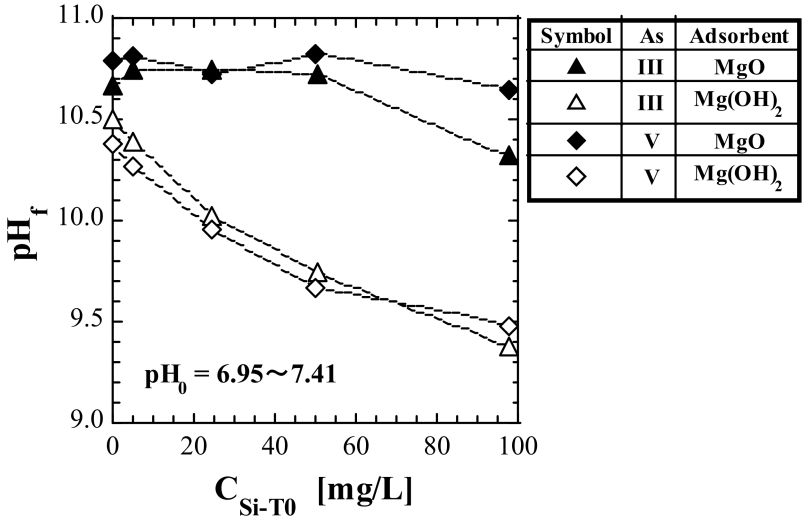


Figure 1. pH values of eluates versus initial total Si-normalized concentration.

3.2. As Concentration in Eluate

Table 5 lists the As concentration (C_{AS}) of each eluate obtained in the shaking tests. Figure 2 plots the C_{AS} value against the $C_{Si\text{-}T0}$ value. The test results for As(V) reported in a previous study [34] are also shown in Table 5 and Figure 2. For both MgO and $Mg(OH)_2$ containing As(III), the C_{AS} values tended to decrease slightly as the $C_{Si\text{-}T0}$ value increased from 0 to 50 mg/L, whereas it increased very slightly at $C_{Si\text{-}T0}$ = 100 mg/L. Overall, the C_{AS} values of the eluents obtained from both adsorbents containing As(III) tended to decrease slightly with an increase in $C_{Si\text{-}T0}$. In contrast, the C_{AS} values of the eluates obtained from $Mg(OH)_2$ containing As(V) increased obviously with an increase in $C_{Si\text{-}T0}$ (Figure 2). The C_{AS} values of the eluates obtained from MgO containing As(V) also tended to increase slightly with an increase in $C_{Si\text{-}T0}$ (Table 5).

Table 5. As concentrations in eluates (C_{AS}).

	$C_{Si\text{-}T0}$ (mg/L)		0	5	25	50	100
No.	**Adsorbent**	**As(Valence)**			C_{AS} (mg/L)		
(1)	MgO	As(III)	0.108	0107	0.043	0.030	0.061
(2)	$MgOH)_2$	As(III)	0.503	0.490	0.432	0.383	0.395
(3) [1]	MgO	As(V)	0.000	0.000	0.000	0.001	0.010
(4) [1]	$Mg(OH)_2$	As(V)	0.012	0.028	0.265	0.677	1.89

[1] The values of No. (3) and (4) are from Sugita et al. (2017) [34].

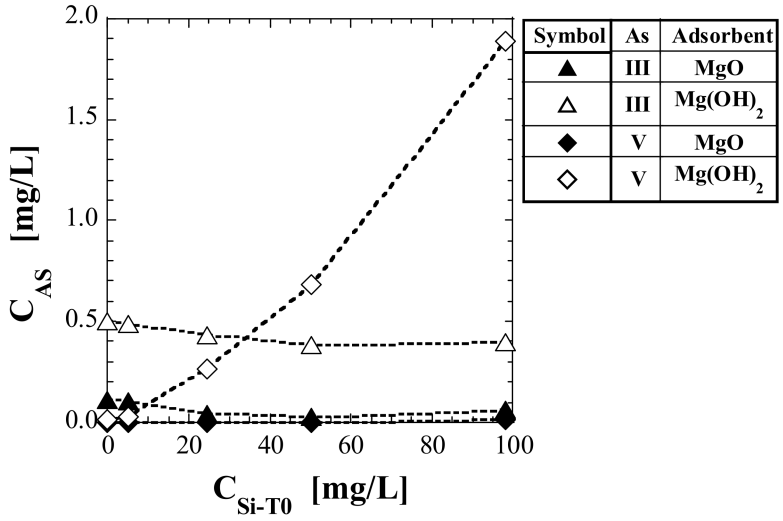


Figure 2. As concentrations in eluates versus initial total Si-normalized concentration.

3.3. Mg Concentration in Eluate

Table 6 lists the Mg concentration (C_{Mg}) of each eluate obtained in the shaking tests. Figure 3 presents a plot of C_{Mg} against $C_{Si\text{-}T0}$. The test results for As(V) reported in our previous study [34] are also shown in Table 6 and Figure 3.

Table 6. Mg concentrations in eluates (C_{Mg}).

	$C_{Si\text{-}T0}$ (mg/L)		0	5	25	50	100
No.	**Adsorbent**	**As(Valence)**			C_{Mg} (mg/L)		
(1)	MgO	As(III)	11.9	13.7	17.2	18.9	21.3
(2)	$Mg(OH)_2$	As(III)	9.1	9.7	11.5	13.3	14.8
(3) [1]	MgO	As(V)	26.9	21.0	20.8	26.7	24.7
(4) [1]	$Mg(OH)_2$	As(V)	10.7	10.7	12.9	15.1	16.7

[1] The values of No. (3) and (4) are from Sugita et al. (2017) [34].

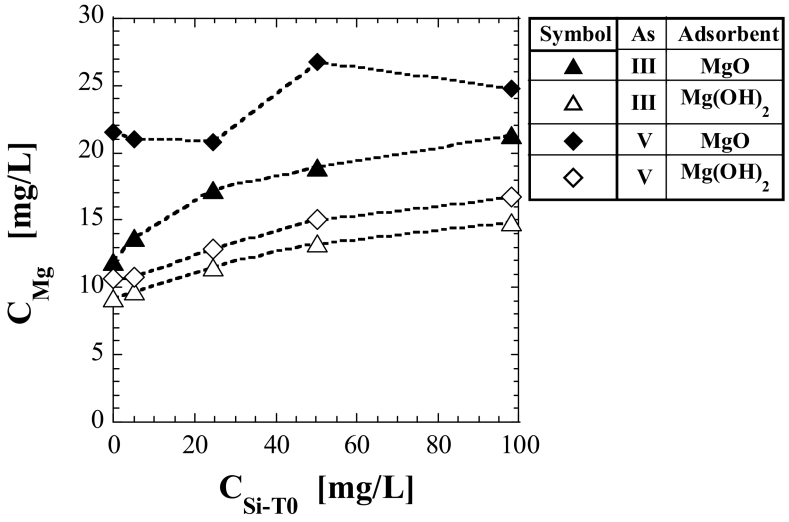


Figure 3. Mg concentrations in eluates versus initial total Si-normalized concentration.

For MgO containing As(V), the C_{Mg} values of the eluates did not change significantly when the $C_{Si\text{-}T0}$ value was between 0 and 25 mg/L, and the C_{Mg} values were lower than those when the $C_{Si\text{-}T0}$ value was 50–100 mg/L. Overall, for the Mg-based adsorbents, the C_{Mg} values tended to increase with an increase in $C_{Si\text{-}T0}$. For both MgO and $Mg(OH)_2$

containing As(III), the C_{Mg} values of the eluates were clearly lower than those for MgO and $Mg(OH)_2$ containing As(V). In addition, for both As(III) and As(V), the C_{Mg} values of the eluates obtained from MgO were higher than those obtained from $Mg(OH)_2$.

3.4. Total Si-Normalized Concentration in Eluate

Table 7 lists the total Si-normalized concentration ($C_{Si\text{-}T}$) of each eluate obtained in the shaking tests. Figure 4 plots $C_{Si\text{-}T}$ against $C_{Si\text{-}T0}$. The test results for As(V) reported in our previous study [34] are also shown in Table 7 and Figure 4. The 1:1 line, which is the straight line of $C_{Si\text{-}T}/C_{Si\text{-}T0} = 1$, is also shown in Figure 4. All data are plotted below the straight line, indicating that some of the silicic acid species dissolved in the liquid phase were adsorbed or precipitated and removed from the liquid phase. For both As(III) and As(V), the $C_{Si\text{-}T}$ values of the eluates obtained from MgO were lower than those obtained from $Mg(OH)_2$. The $C_{Si\text{-}T}$ values of the eluates from MgO containing As(III) were higher than those from MgO containing As(V), whereas the $C_{Si\text{-}T}$ values of eluates from $Mg(OH)_2$ containing As(III) and $Mg(OH)_2$ containing As(V) were similar.

Table 7. Total Si-normalized concentrations in eluates ($C_{Si\text{-}T}$).

$C_{Si\text{-}T0}$ (mg/L)			0	5	25	50	100
No.	**Adsorbent**	**As(Valence)**	$C_{Si\text{-}T}$ (mg/L)				
(1)	MgO	As(III)	0.00	0.08	0.95	3.90	18.3
(2)	$Mg(OH)_2$	As(III)	0.00	0.77	13.1	35.4	72.2
(3) [1]	MgO	As(V)	0.00	0.15	0.15	1.41	3.24
(4) [1]	$Mg(OH)_2$	As(V)	0.00	2.43	17.1	40.3	70.2

[1] The values of No. (3) and (4) are from Sugita et al. (2017) [34].

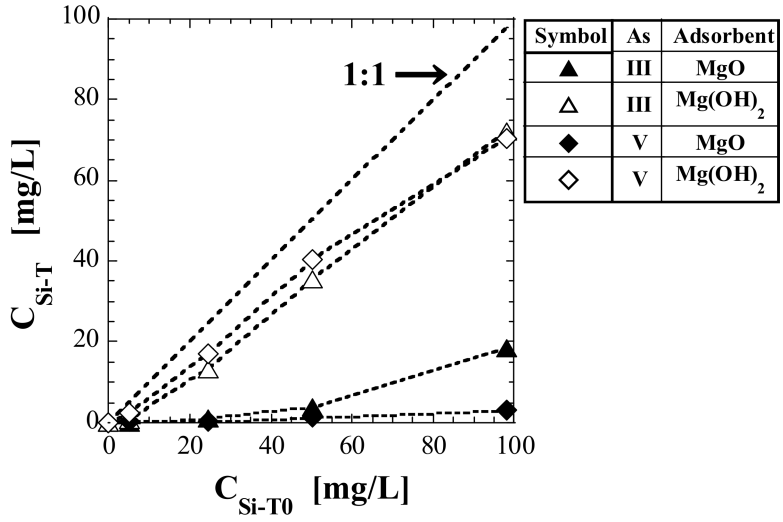


Figure 4. Total Si-normalized concentrations in eluates versus initial total Si-normalized concentration.

3.5. Reproducibility of Experimental Data

The shaking tests using the spent adsorbents (MgO and $Mg(OH)_2$) containing As(III) and the silicic acid solution at $C_{Si\text{-}T0}$ = 50 mg/L were repeated three times. The relative standard errors associated with the pH_f, C_{AS}, C_{Mg}, and $C_{Si\text{-}T}$ values were 0.04%, 4.9%, 0.5%, and 1.9%, respectively, for MgO, and 0.01%, 3.8%, 0.4%, and 2.4%, respectively, for $Mg(OH)_2$. Based on these results, it was confirmed that the reproducibility of the experimental data was good.

4. Discussion

4.1. Relative Evaluation Using As Leaching Ratio

The As content varied slightly between the two types of spent adsorbents (Table 3). As in previous studies [12,13,34], the As leaching ratio, E_{AS} (%), was calculated and used for the evaluation:

$$E_{AS} = C_{AS}/(Q_{AS} \times W_{SP}/V) \times 100 \quad (7)$$

where W_{SP} is the amount of spent adsorbent added to the test solvent (g), and V is the liquid volume of the test solvent (L); hence, W_{SP}/V is the amount of spent adsorbent added per unit volume of test solvent (g/L).

Table 8 lists the E_{AS} values obtained using Equation (7). Figure 5 shows a plot of E_{AS} against $C_{Si\text{-}T0}$. For comparison with As(III), the E_{AS} values for spent Mg-based adsorbents containing As(V) reported in our previous study [34] are also shown in Table 8 and Figure 5. For MgO and $Mg(OH)_2$ containing As(III), the E_{AS} values both decreased slightly with an increase in $C_{Si\text{-}T0}$ from 0 to 50 mg/L, before increasing slightly at 100 mg/L. The E_{AS} values of MgO containing As(III) were higher than those for MgO containing As(V). The E_{AS} values of MgO containing As(V) were extremely low (<0.01%) at $C_{Si\text{-}T0}$ = 0–50 mg/L, because very little As leached from the spent adsorbents (Table 8). However, the E_{AS} value of MgO containing As(V) at $C_{Si\text{-}T0}$ = 100 mg/L was an order of magnitude higher than those at 0–50 mg/L. Different to the other three adsorbents, the E_{AS} values of $Mg(OH)_2$ containing As(V) increased considerably, by two orders of magnitude, with an increase in $C_{Si\text{-}T0}$ (Figure 5).

Table 8. Values of As leaching ratio (E_{AS}).

$C_{Si\text{-}T0}$ (mg/L)			0	5	25	50	100
No.	**Adsorbent**	**As(Valence)**	E_{AS} (%)				
(1)	MgO	As(III)	1.24	1.22	0.50	0.34	0.69
(2)	$Mg(OH)_2$	As(III)	5.97	5.85	5.12	4.55	4.71
(3) [1]	MgO	As(V)	>0.01	>0.01	>0.01	>0.01	0.12
(4) [1]	$Mg(OH)_2$	As(V)	0.14	0.34	3.13	7.98	22.1

[1] The values of No. (3) and (4) are from Sugita et al. (2017) [34].

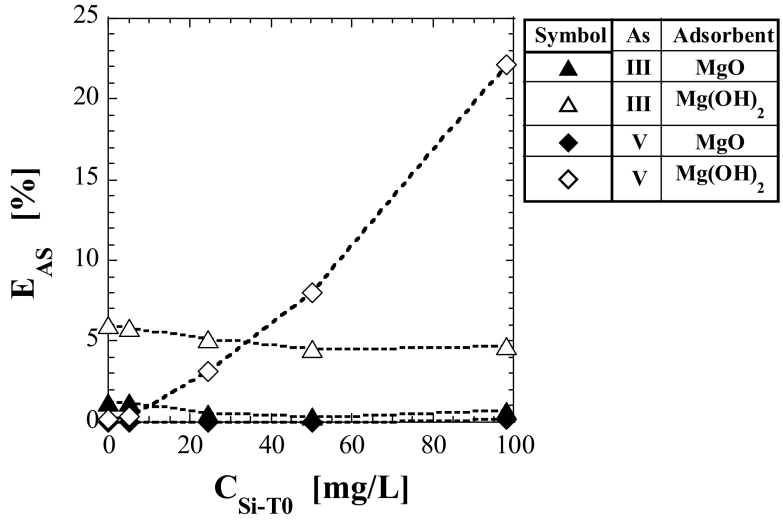


Figure 5. As leaching ratios of adsorbents versus initial total Si-normalized concentration.

4.2. Dissolved Forms of Siliacic Acid in Liquid

Similar to previous studies [12,13,34], the dissolved forms of silicic acid in liquid were considered based on the dissociation formulae of silicic acid:

$$H_4SiO_4 \longleftrightarrow H_3SiO_4^- + H^+ \quad (8)$$

$$H_3SiO_4^- \longleftrightarrow H_2SiO_4^{2-} + H^+ \quad (9)$$

When the equilibrium constants of the dissociation Formulas (8) and (9) are denoted as Ka_1 and Ka_2, respectively, the following equations are applicable:

$$[H_3SiO_4^-]/[H_4SiO_4] = 10 \exp (pH - pKa_1) \quad (10)$$

$$[H_2SiO_4^{2-}]/[H_3SiO_4^-] = 10 \exp (pH - pKa_2) \quad (11)$$

where the units of the applicable molecular formula are mol/L, $pKa_1 = 9.86$, and $pKa_2 = 13.1$ (25 °C) [37].

The pH_f values obtained in the shaking tests for As(III) ranged from 9.38 to 10.75 (see Table 4). Substituting these values into Equation (10) yields values in the range of 0.33–7.75. In addition, substituting the pH_f values into Equation (11) yields values of less than 0.005, indicating that the main dissolved forms were $H_3SiO_4^-$ (a monovalent ion) and H_4SiO_4 (a non-valent molecule), while $H_2SiO_4^{2-}$ did not exist. In our previous study on As(V), we also found that the main dissolved forms were $H_3SiO_4^-$ and H_4SiO_4 [34]. In addition, previous studies have reported that, in the test solvent before adding the spent adsorbent, the ionization ratio of silicic acid was 0.1–0.4%, and most of the silicic acid existed as an uncharged monosilicic acid [13,34].

4.3. Dissolved Forms of Arsenous Acid in Liquid

As in the case of the spent Ca-based adsorbents containing As(III) [12], the As(III) in spent Mg-based adsorbents is presumed to be adsorbed (immobilized) on the solid surface as follows: Solid-O-Mg-O-As$(OH)_2$, followed by a reaction wherein As(III) on the surface of the adsorbent is desorbed in a neutral or alkaline solution, as represented by Equations (12) and (13), respectively.

$$\text{Solid-O-Mg-O-As(OH)}_2 + H_2O \rightarrow \text{Solid-O-Mg-OH} + \text{As(OH)}_3 \quad (12)$$

$$\text{Solid-O-Mg-O-As(OH)}_2 + OH^- \rightarrow \text{Solid-O-Mg-OH} + \text{As(OH)}_2O^- \quad (13)$$

In addition, the dissolved form of As(III) leached from the spent adsorbent is represented by the following dissociation reactions for arsenous acid:

$$H_3AsO_3 \longleftrightarrow H_2AsO_3^- + H^+ \quad (14)$$

$$H_2AsO_3^- \longleftrightarrow HAsO_3^{2-} + H^+ \quad (15)$$

$$HAsO_3^{2-} \longleftrightarrow AsO_3^{3-} + H^+ \quad (16)$$

where $pKa_1 = 9.1$, $pKa_2 = 12.1$, and $pKa_3 = 13.4$ (25 °C) [37]. In this study, as $pH_f < pKa_3$, the abundance of AsO_3^{3-} was extremely small and negligible. The values of pKa_1 and pKa_2 were applied to Equations (17) and (18), corresponding to Equations (14) and (15), respectively.

$$[H_2AsO_3^-]/[\,H_3AsO_3] = 10 \exp (pH - pKa_1) \quad (17)$$

$$[HAsO_3^{2-}]/[\,H_2AsO_3^-] = 10 \exp (pH - pKa_2) \quad (18)$$

Then, substituting the pH_f values of 9.38–10.75, the values of $(H_2AsO_3^-)/(H_3AsO_3)$ and $(HAsO_3^{2-})/(H_2AsO_3^-)$ were calculated to be 1.90–44.6 and 0.002–0.045, respectively. Based on the results, the main dissolved form of As leached from the spent Mg-based adsorbents was presumed to be $H_2AsO_3^-$, a dihydrogen arsenite ion. In our previous

study on As(V), we found that the main dissolved form was $HAsO_4^{2-}$, a hydrogen arsenate ion [34]. Similar to our previous findings [34], it is possible that the valence of As may have changed during the shaking tests; however, in the present study, neither oxidizing nor reducing agents were used, and the shaking time was only one day. In addition, Tresintsi et al. (2014) and Opiso et al. (2010) reported that the valence of adsorbed As did not change from the original valence [31,33]. Therefore, we assumed that the valence of As did not change in our study.

4.4. Stoichiometric Considerations on Spent Mg-Based Adsorbents

In this section, similar to previous studies [12,13,34], stoichiometric considerations were made using the values obtained by converting the mass-based concentration C_X (mg/L) to the molar-based concentration M_X (mmol/L).

4.4.1. Relationship between Dissolved Components and pH of Eluate

The dissolved components in an eluate are expected to be considerably affected by pH_f. In Figures 6–8, M_{AS}, M_{Mg} and $M_{Si\text{-}T}$ are plotted against pH_f. In Figure 7, the solubility curve of pure $Mg(OH)_2$, which was calculated using the solubility product = 1.1×10^{-11} [38], is also shown.

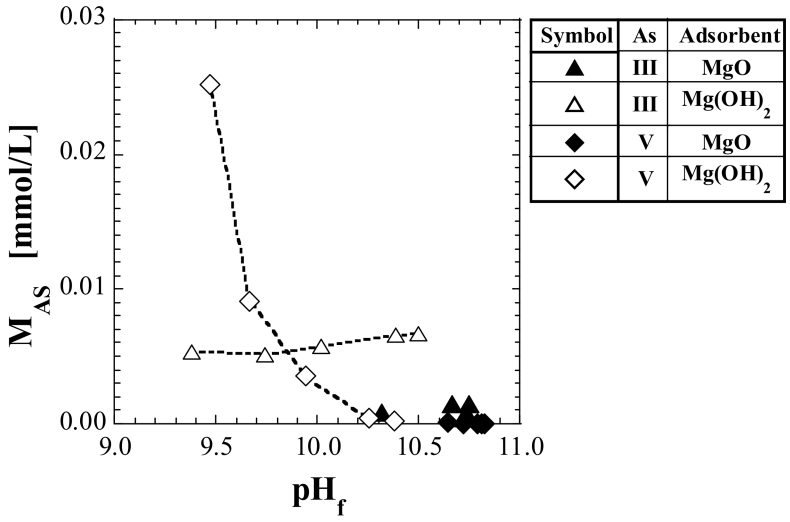


Figure 6. Plot of M_{AS} against pH_f.

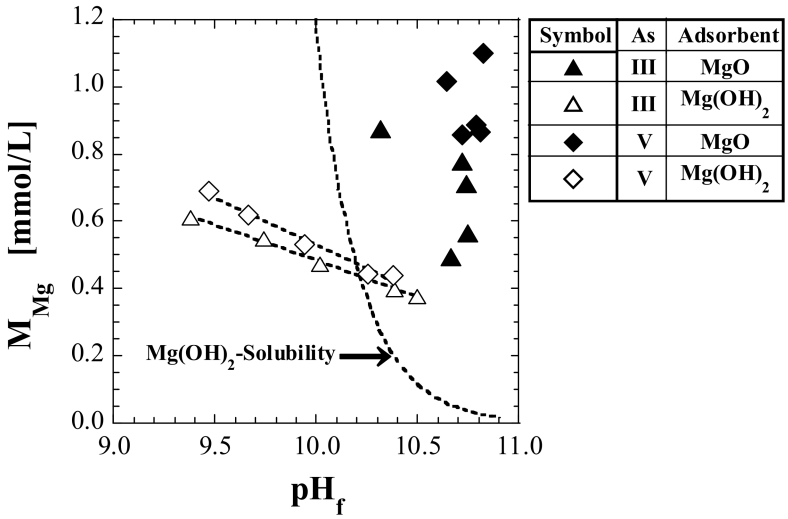


Figure 7. Plot of M_{Mg} versus pH_f.

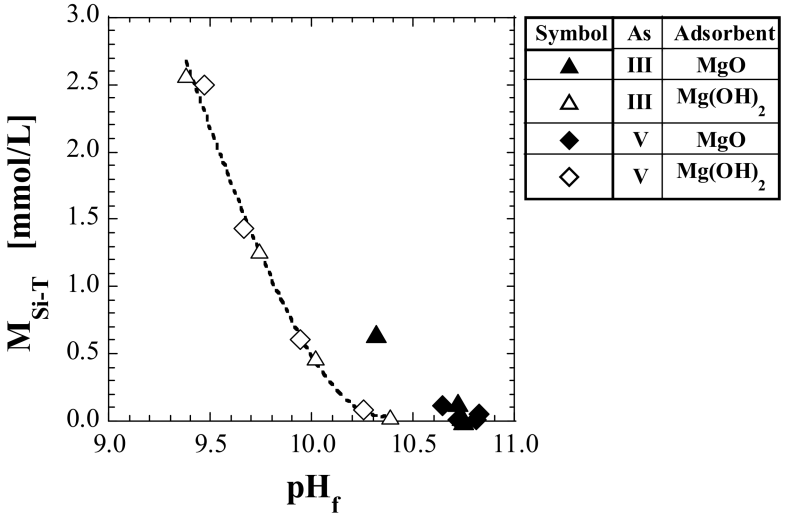


Figure 8. Plot of $M_{\text{Si-T}}$ versus pH_{f}.

As shown in Figure 6, the M_{AS} value for $Mg(OH)_2$ containing As(V) decreased drastically with increasing pH_{f}. For the other adsorbents, there was no clear correlation between M_{AS} and pH_{f}. Although it is usually presumed that As is more likely to leach in an alkaline region (due to the ion exchange reaction with hydroxide ions), no such tendency was observed in this study.

As shown in Figure 7, none of the plots for the Mg-based adsorbents fitted into the $Mg(OH)_2$ solubility curve. For $Mg(OH)_2$ containing As(III) and $Mg(OH)_2$ containing As(V), M_{Mg} was inversely proportional to pH_{f}; therefore, it can be presumed that a correlation exists between M_{Mg} and the OH^- concentration.

As shown in Figure 8, the $M_{\text{Si-T}}$ value tended to decrease with increasing pH_{f}. In particular, for $Mg(OH)_2$, the values are plotted on a curve, regardless of the valence of As. It is generally known that the solubility of amorphous silica increases with increasing pH; however, the results obtained in this study were the opposite. Therefore, factors other than the solubility of amorphous silica affected the $M_{\text{Si-T}}$ value.

From the above results, for $Mg(OH)_2$, M_{Mg} and $M_{\text{Si-T}}$ can be considered to correlate with pH_{f} (i.e., OH^-). When $Mg(OH)_2$ releases one Mg^{2+} ion, it usually releases two OH^- ions.

$$Mg(OH)_2 \rightarrow Mg^{2+} + 2OH^- \quad (19)$$

In addition, the same applies to cases wherein it is assumed that MgO is hydrated to produce $Mg(OH)_2$, as shown in Equation (20), and then dissolved.

$$MgO + H_2O \rightarrow Mg(OH)_2 \quad (20)$$

However, when adsorbed on the surface of the $Mg(OH)_2$ adsorbent, OH^- is not released.

$$\text{Solid-O-Mg-OH} + H_4SiO_4 \rightarrow \text{Solid-O-Mg-O-Si(OH)}_3 + H_2O \quad (21)$$

When $H_3SiO_4^-$ is adsorbed, OH^- is released, but as the OH^- is offset by the H^+ dissociated from H_4SiO_4, the balance of OH^- in the system is virtually zero.

$$\text{Solid-O-Mg-OH} + H_3SiO_4^- \rightarrow \text{Solid-O-Mg-O-Si(OH)}_3 + OH^- \quad (22)$$

However, as described in Section 4.2, some of the silicic acid remaining in the eluate is present as $H_3SiO_4^-$. This is easy to understand when Equation (8) is rewritten as Equation (23).

$$H_4SiO_4 + OH^- \longleftrightarrow H_3SiO_4^- + H_2O \quad (23)$$

Assuming that the change in OH^- accompanying the leaching of As is negligible, because the amount of As leaching is very small, the value obtained by adding the abundance of $H_3SiO_4^-$ in the eluate to the difference between the OH^- concentration at pH_0 and pH_f should be equivalent to the amount of OH^- produced by the dissolution of $Mg(OH)_2$.

The pH_0 and pH_f values converted to OH^- concentrations are denoted as $[OH^-]_0$ and $[OH^-]_f$, respectively. The difference between pH_0 and pH_f (i.e., $pH_f - pH_0$) is denoted as $\Delta[OH^-]_f$. In addition, the $H_3SiO_4^-$ concentration in the eluate is denoted as $[H_3SiO_4^-]_f$. The units for these were mmol/L. Assuming that the amount of OH^- released by the dissolution of $Mg(OH)_2$ is twice that of Mg^{2+}, $\Delta[OH^-]_f + [H_3SiO_4^-]_f$ is plotted against $2M_{Mg}$ in Figure 9. If the above assumptions are correct, the data should plot on a 1:1 line, but all the data plot below the line. This may be due to the consumption of OH^- by the absorption of CO_2 from the air. For comparison, $\Delta[OH^-]_f + [H_3SiO_4^-]_f$ is plotted against M_{Mg} in Figure 10.

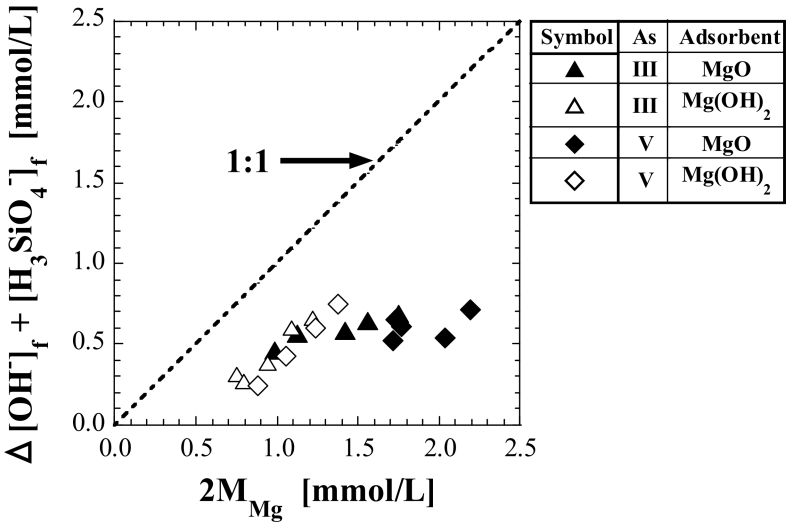


Figure 9. Plot of $\Delta[OH^-]_f + [H_3SiO_4^-]_f$ versus $2M_{Mg}$.

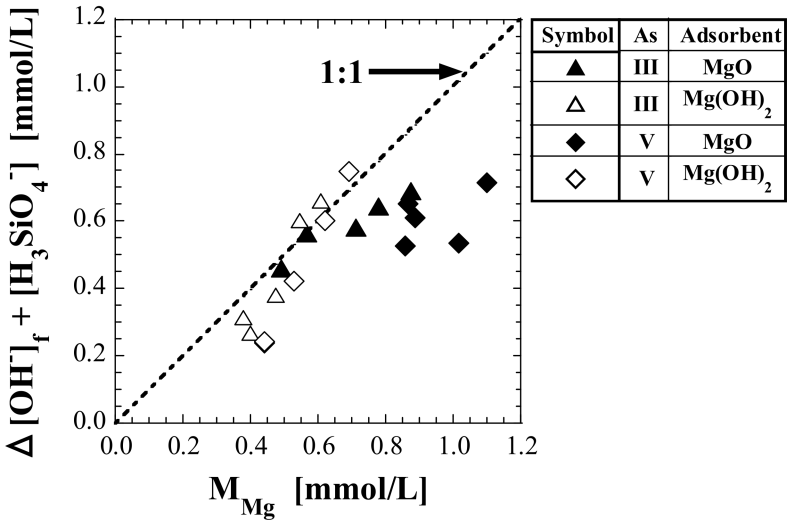


Figure 10. Plot of $\Delta[OH^-]_f + [H_3SiO_4^-]_f$ versus M_{Mg}.

In Figure 10, many data are plotted near the 1:1 line, which may indicate that the dissolved form of Mg was $Mg(OH)^+$ rather than Mg^{2+}.

$$Mg(OH)_2 \rightarrow Mg(OH)^+ + OH^- \quad (24)$$

Alternatively, Mg^{2+} and OH^- could have been released at a 1:1 ratio, primarily by the dissolution of the surface layer portion of the adsorbent, as expressed by Equation (25):

$$\text{Solid-O-Mg-OH} \rightarrow \text{Solid-O}^- + Mg^{2+} + OH^- \quad (25)$$

To understand these issues correctly, future studies should measure the surface charge of the adsorbents and perform more detailed chemical equilibrium calculations.

4.4.2. Relationship between Mg Leaching and Silicic Acid Adsorption

Similar to previous studies [12,13,34], the $M_{Si\text{-}T}$ value at $C_{Si\text{-}T0}$ = 0 mg/L was denoted as $M_{Si\text{-}T0}$ in this study, and the difference between $M_{Si\text{-}T0}$ and $M_{Si\text{-}T}$ (i.e., $M_{Si\text{-}T0} - M_{Si\text{-}T}$) was denoted as $\Delta M_{Si\text{-}T}$. Likewise, the M_{Mg} value at $C_{Si\text{-}T0}$ = 0 mg/L was denoted as M_{Mg0}, and the difference between M_{Mg0} and M_{Mg} (i.e., $M_{Mg0} - M_{Mg}$) was denoted as ΔM_{Mg}.

Figure 11 shows a semi-log plot of $-\Delta M_{Mg}$ versus $\Delta M_{Si\text{-}T}$. An increase in the value of $-\Delta M_{Mg}$ indicates an increase in the amount of leached Mg, while an increase in the $\Delta M_{Si\text{-}T}$ value indicates an increase in the amount of adsorbed Si.

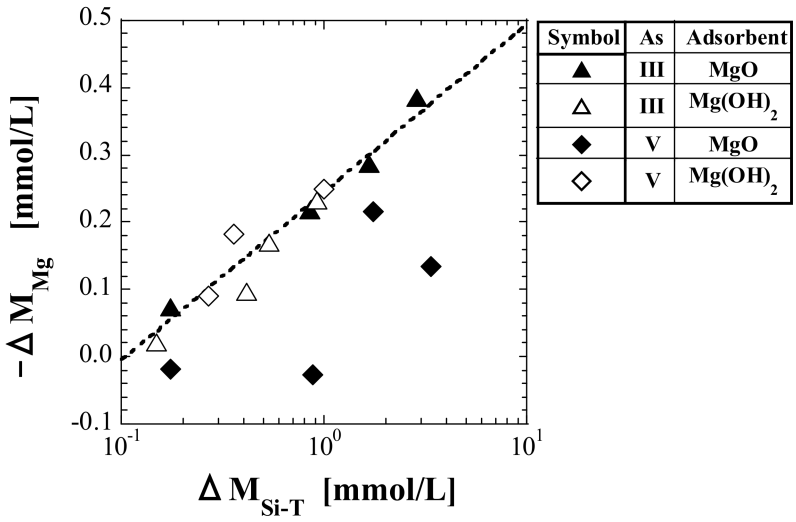


Figure 11. Semi-log plot of $-\Delta M_{Mg}$ versus $M_{Si\text{-}T}$.

Except for MgO containing As(V), a proportional correlation was found between the values of $-\Delta M_{Mg}$ and the logarithmic values of $\Delta M_{Si\text{-}T}$, which may be represented by a single curve. The approximate expression of the curve obtained using the data excluding MgO containing As(V) is shown below:

$$-\Delta M_{Mg} = 0.245 + 0.250 \log(\Delta M_{Si\text{-}T}) \quad (26)$$

The correlation coefficient was 0.975. This high correlation indicates that Mg was leached from the Mg-based adsorbents by the adsorption of silicic acid species, and that the accompanying reaction mechanism of Mg leaching was the same, except for MgO containing As(V). Thus, the adsorption mechanism of silicic acid on the surface of the Mg-based adsorbents (Equation (27), which releases Mg^{2+}, and Equation (21), which does not release Mg^{2+}) can be considered.

$$\text{Solid-O-Mg-OH} + H_4SiO_4 \rightarrow \text{Solid-O-Si(OH)}_3 + Mg^{2+} + 2OH^- \quad (27)$$

From Equation (26), it can be seen that the reaction of Equation (21) is predominant over that of Equation (27). In addition, for the MgO adsorbent containing As(V), when $\Delta M_{Si\text{-}T}$ was less than 1 mmol/L, the reaction of Equation (27) hardly occurred because the $-\Delta M_{Mg}$ value was negative.

Opiso et al. [33] confirmed the formation of magnesium silicate in a Mg–Si–Al system, but not in a Mg–Si system. As our experiments were also an aluminum-free Mg–Si system, the formation of magnesium silicate did not occur. The fact that there was no decrease in $-\Delta M_{Mg}$ with the increase in $\Delta M_{Si\text{-}T}$ also supports the above hypothesis.

4.4.3. Relationship between As Leaching and Silicic Acid Adsorption

The M_{AS} value at $C_{Si\text{-}T0} = 0$ mg/L was denoted as M_{AS0}, and the difference between M_{AS0} and M_{AS} (i.e., $M_{AS0} - M_{AS}$) was denoted as ΔM_{AS} in this study. Figure 12 plots $-\Delta M_{AS}$ against $\Delta M_{Si\text{-}T}$. The increase in the value of $-\Delta M_{AS}$ indicates an increase in the leaching amount of As. For the $Mg(OH)_2$ adsorbent containing As(V), $-\Delta M_{AS}$ increased with an increase in $\Delta M_{Si\text{-}T}$. However, for the other adsorbents, no correlation was found between $-\Delta M_{AS}$ and $\Delta M_{Si\text{-}T}$.

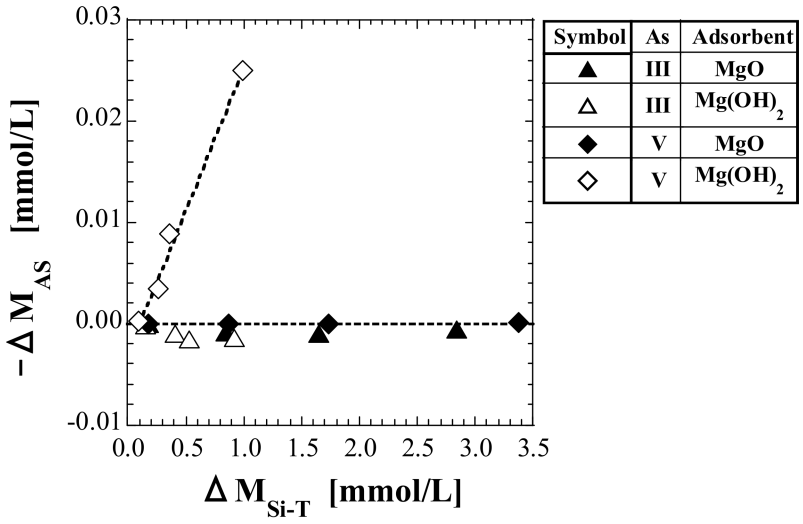


Figure 12. Plot of $-\Delta M_{AS}$ versus M_{Mg}.

The approximate expression of the straight line obtained using the data for the $Mg(OH)_2$ adsorbent containing As(V) is shown below.

$$-\Delta M_{AS} = -0.00256 + 0.0280\Delta M_{Si\text{-}T} \quad (28)$$

The correlation coefficient was 0.994, indicating that the adsorbed As(V) on the $Mg(OH)_2$ adsorbent was released by ion exchange with silicic acid species according to Equation (13).

$$\text{Solid-Mg-O-AsO(OH)}_2 + H_3SiO_4^- \rightarrow \text{Solid-Mg-O-Si(OH)}_3 + H_2AsO_4^- \quad (29)$$

In other words, Equation (28) indicates that one As(V) was desorbed by the adsorption of approximately 36 (=1/0.028) silicic acid species.

For the MgO and $Mg(OH)_2$ adsorbents containing As(III), $-\Delta M_{AS}$ was negative. This phenomenon has also been reported for spent Ca-based adsorbents, and it is considered that the coating effect due to the adsorption of silicic acid species makes it difficult to desorb As [13]. The coating effect suggests that silicic acid layers are formed on the surfaces of the adsorbent.

4.4.4. Comparison of Spent Mg-Based and Ca-Based Adsorbents

In this study, the effect of silicic acid on the leaching behavior of As from spent Mg-based adsorbents differed considerably from that observed for Ca-based adsorbents in previous studies [12,13]. In the case of spent Ca-based adsorbents, previous studies reported that the E_{AS} values decreased drastically with an increase in $C_{Si\text{-}T0}$, regardless of

the valence of the As adsorbed on the adsorbents [12,13]. For MgO containing As(V) and $Mg(OH)_2$ containing As(V), the E_{AS} values increased slightly and drastically, respectively, with an increase in $C_{Si\text{-}T0}$ [34], whereas the E_{AS} values decreased slightly for MgO and $Mg(OH)_2$ containing As(III). When the $C_{Si\text{-}T0}$ increased from 0 to 100 mg/L, the E_{AS} value reduced from 1.24% to 0.69% for MgO containing As(III), from 5.97% to 4.71% for $Mg(OH)_2$ containing As(III), from 8.00% to 0.695% for CaO containing As(III), and from 8.89% to 0.670% for $Ca(OH)_2$ containing As(III). In contrast, the E_{AS} value changed from less than 0.01% to 0.12% for MgO containing As(V), from 0.14% to 22.1% for $Mg(OH)_2$ containing As(V), from 16.5% to 3.78% for CaO containing As(V), and 7.43% to 1.94% for $Ca(OH)_2$ containing As(V) (see Table 8 in this paper and Table 9 in Sugita et al. (2021) [12]). Therefore, based on EAS as the evaluation criterion, when a high silicic acid concentration is expected in the liquid with which a spent adsorbent comes into contact in the disposal environment, the adsorbents used to treat As(III) and As(V), respectively, should be prioritized as follows:

For treating As(III), MgO > $Ca(OH)_2$ = CaO > $Mg(OH)_2$.

For treating As(V), MgO > $Ca(OH)_2$ >> CaO >> $Mg(OH)_2$.

Therefore, considering the risk of As leaching from spent adsorbents after disposal, MgO is the best adsorbent, regardless of the valence of As. In some cases, $Ca(OH)_2$ may also be recommended to achieve a lower cost. In addition, it has also been reported that the leaching amount of Ca^{2+} from Ca-based adsorbents decreased with an increase in $C_{Si\text{-}T0}$ [12,13], whereas the leaching amount of Mg^{2+} from the Mg-based adsorbents in this study increased with an increase in $C_{Si\text{-}T0}$. This difference probably relates to the formation and precipitation of calcium silicate species in the case of Ca-based adsorbents, whereas magnesium silicate species did not form or precipitate in the case of the Mg-based adsorbents reported here, as mentioned in Section 4.4.2.

5. Conclusions

Previous studies [12,13,34] have reported the effects of silicic acid on the environmental stabilities of the spent Ca-based adsorbents containing As(V) and As(III), and spent Mg-based adsorbents containing As(V). In this study, the effects of silicic acid on the environmental stabilities of two spent Mg-based adsorbents containing As(III) were examined.

In our previous study, we found that the leaching amount of As from spent Mg-based adsorbents containing As(V) tended to increase with an increase in the initial silicic acid concentration [34]. In contrast, in the present study, the leaching amount of As from spent Mg-adsorbents containing As(III) decreased slightly with an increase in the initial silicic acid concentration. For MgO and $Mg(OH)_2$ containing As(III), the amount of leached Mg was clearly lower than that observed for MgO and $Mg(OH)_2$ containing As(V). In addition, compared with $Mg(OH)_2$ adsorbents containing As(III) or As(V), the amount of leached Mg was higher, and the silicic acid concentration in the eluate was lower for MgO adsorbents containing As(III) or As(V). For MgO containing As(III), the silicic acid concentration in the eluate was higher than that for MgO containing As(V), whereas approximately the same silicic acid concentrations were observed for $Mg(OH)_2$ containing As(III) and $Mg(OH)_2$ containing As(V).

In our previous study, we found that the As leaching ratio for As(V) increased from less than 0.01% to 0.12% for MgO and from 0.14% to 22.1% for $Mg(OH)_2$ when the initial total Si-normalized concentration increased from 0 to 100 mg/L [34]. Conversely, in this study, the As leaching ratio for As(III) decreased from 1.24% to 0.69% for MgO and from 5.97% to 4.71% for $Mg(OH)_2$ when the initial total Si-normalized concentration increased from 0 to 100 mg/L. For the spent Mg-based adsorbents containing As(V), As leaching probably occurred as a result of the ion exchange reaction with silicic acid species, whereas this reaction hardly occurred for the spent Mg-based adsorbents containing As(III).

Considering the risk of As leaching from spent adsorbents after disposal, among the Mg-based and Ca-based adsorbents discussed in this work, the best adsorbent was found to be MgO, regardless of the valence of As. With respect to environmental and social

sustainability, it is important to select an adsorbent based on its As removal performance and environmental stability after disposal.

Author Contributions: Conceptualization, H.S.; methodology, H.S. and J.H.; formal analysis, H.S. and J.H.; investigation, T.O. and H.S.; resources, H.S., M.Z., and J.H.; data curation, T.O. and H.S.; writing—original draft preparation, H.S. and T.O.; writing—review and editing, H.S., T.O., M.Z., J.H. and Y.K.; supervision, H.S. and M.Z.; project administration, M.Z. and Y.K.; funding acquisition, M.Z., Y.K. and H.S. All authors have read and agreed to the published version of the manuscript.

Funding: This research received no external funding.

Institutional Review Board Statement: Not applicable.

Informed Consent Statement: Not applicable.

Data Availability Statement: Data that support the findings of this study are available from the corresponding authors upon reasonable request.

Conflicts of Interest: The authors declare no conflict of interest.

References

1. Podgorski, J.; Berg, M. Global threat of arsenic in groundwater. *Science* **2020**, *368*, 845–850. [CrossRef]
2. Shaji, E.; Santosh, M.; Sarath, K.V.; Prakash, P.; Deepch, V.; Divy, B.V. Arsenic contamination of groundwater: A global synopsis with focus on the Indian Peninsula. *Geosci. Front.* **2021**, *13*, 101079. [CrossRef]
3. The World Health Organization (WHO). *Guidelines for Drinking-Water Quality, Fourth Edition*; WHO: Tarxien, Malta, 2011; Arsenic, 315-318; Available online: https://apps.who.int/iris/bitstream/handle/10665/44584/9789241548151_eng.pdf (accessed on 27 December 2021).
4. Wirth, G.S.; Gieskes, J.M. The Initial kinetics of the dissolution of vitreous silica in aqueous media. *J. Colloid Interface Sci.* **1979**, *68*, 492–500. [CrossRef]
5. Rothbaum, H.P.; Rohde, A.G. Kinetics of silica polymerization and deposition from dilute solutions between 5 and 180 °C. *J. Colloid Interface Sci.* **1979**, *71*, 533–559. [CrossRef]
6. Marshall, W.L. Amorphous silica solubilities I. Behavior in aqueous salt solutions at 25 °C. *Geochim. Cosmochim. Acta* **1980**, *44*, 907–913. [CrossRef]
7. Bohlmann, E.G.; Mesmer, R.E.; Berlinski, P. Kinetics of silica deposition from simulated geothermal brines. *Soc. Pet. Eng. J.* **1980**, *50*, 239–248. [CrossRef]
8. Weres, O.; Yee, A.; Tsao, L. Kinetics of silica polymerization. *J. Colloid Interface Sci.* **1981**, *84*, 379–402. [CrossRef]
9. Fleming, B.A.; Crerar, D.A. Silicic acid ionization and calculation of silica solubility at elevated temperature and pH application to geothermal fluid processing and reinjection. *Geothermics* **1982**, *11*, 15–29. [CrossRef]
10. Fournier, R.O.; Marshall, W.L. Calculation of amorphous silica solubilities at 25° to 300 °C and apparent cation hydration numbers in aqueous salt solutions using the concept of effective density of water. *Geochim. Cosmochim. Acta* **1983**, *47*, 587–596. [CrossRef]
11. Fleming, B.A. Kinetics of reaction between silicic acid and amorphous silica surfaces in NaCl solutions. *J. Colloid Interface Sci.* **1986**, *110*, 40–64. [CrossRef]
12. Sugita, H.; Oguma, T.; Hara, J.; Zhang, M.; Kawabe, Y. Effects of silicic acid on leaching behavior of arsenic from spent calcium-based adsorbents with arsenite. *Sustainability* **2021**, *13*, 12937. [CrossRef]
13. Sugita, H.; Oguma, T.; Zhang, M.; Hara, J.; Kawabe, Y. Effects of silicic acid on environmental stability of spent calcium-based arsenic adsorbents. *J. Jpn. Soc. Civ. Eng. Ser. G Environ. Res.* **2018**, *74*, 493–502. [CrossRef]
14. Ruhaimi, A.H.; Aziz, M.A.A.; Jalil, A.A. Magnesium oxide-based adsorbents for carbon dioxide capture: Current progress and future opportunities. *J. CO_2 Util.* **2021**, *43*, 101357. [CrossRef]
15. Tan, C.; Guo, Y.; Sun, J.; Li, W.; Zhang, J.; Zhao, C.; Lu, P. Structurally improved MgO adsorbents derived from magnesium oxalate precursor for enhanced CO_2 capture. *Fuel* **2020**, *278*, 118379. [CrossRef]
16. Cheng, W.; Fang, L.; Cheng, H.; Li, E.; Zhang, C.; Cheng, F. Formation of $MgCO_3$ $3H_2O$ in the CO_2 mineralization system using $Mg(OH)_2$ as an intermediate at 20 °C. *J. Ind. Eng. Chem.* **2019**, *76*, 215–222. [CrossRef]
17. Wu, S.; Tan, B.T.; Senevirathna, H.L.; Wu, P. Polarization of CO_2 for improved CO_2 adsorption by MgO and $Mg(OH)_2$. *Appl. Surf. Sci.* **2021**, *562*, 150187. [CrossRef]
18. Mohan, S.; Singh, D.K.; Kumar, V.; Hasan, S.H. Modelling of fixed bed column containing graphene oxide decorated by MgO nanocubes as adsorbent for Lead (II) removal from water. *J. Water Process Eng.* **2017**, *17*, 216–228. [CrossRef]
19. Li, B.; Pu, S.; Mandal, S.; Li, M. Viscosity modification enhanced the migration and distribution of colloidal $Mg(OH)_2$ in aquifers contaminated by heavy metals. *Environ. Int.* **2020**, *138*, 105658. [CrossRef]
20. Xiang, J.; Lin, Q.; Yao, X.; Yin, G. Removal of Cd from aqueous solution by chitosan coated MgO-biochar and its in-situ remediation of Cd-contaminated soil. *Environ. Res.* **2021**, *195*, 110650. [CrossRef] [PubMed]

21. Zhao, N.-D.; Wang, Y.; Zou, X.-H.; Yin, W.-M.; Wang, X.-Y.; Guo, Y.-R.; Pan, Q.-J. Fabrication of cellulose@$Mg(OH)_2$ composite filter via interfacial bonding and its trapping effect for heavy metal ions. *Chem. Eng. J.* **2021**, *426*, 130812. [CrossRef]
22. Zhang, Y.; Xu, G.-S.; Xu, M.-D.; Wang, D.-C.; Wang, H.; Zhan, Y.; Jin, Z. Preparation of MgO porous nanoplates modified pumice and its adsorption performance on fluoride removal. *J. Alloys Compd.* **2021**, *884*, 160953. [CrossRef]
23. Falyouna, O.; Bensaida, K.; Maamoun, I.; Ashik, U.P.M.; Tahara, A.; Tanaka, K.; Aoyagi, N.; Sugihara, Y.; Eljamal, O. Synthesis of hybrid magnesium hydroxide/magnesium oxide nanorods [$Mg(OH)_2$/MgO] for prompt and efficient adsorption of ciprofloxacin from aqueous solutions. *J. Clean. Prod.* **2022**, *342*, 130949. [CrossRef]
24. Cao, N.; Zhao, X.; Gao, M.; Li, Z.; Ding, X.; Li, C.; Liu, K.; Du, X.; Li, W.; Feng, J.; et al. Superior selective adsorption of MgO with abundant oxygen vacancies to removal and recycle reactive dyes. *Sep. Purif. Technol.* **2021**, *275*, 119236. [CrossRef]
25. Yunessni, L.A.; Akbari, A. Membrane capsules with hierarchical $Mg(OH)_2$ nanostructures as novel adsorbents for dyeing wastewater treatment in carpet industries. *J. Taiwan Inst. Chem. Eng.* **2017**, *70*, 391–400. [CrossRef]
26. Camacho, J.; Wee, H.-Y.; Kramer, T.A.; Autenrieth, R. Arsenic stabilization on water treatment residuals by calcium addition. *J. Hazard. Mater.* **2009**, *165*, 599–603. [CrossRef] [PubMed]
27. Montes-Hernandeza, G.; Concha-Lozan, N.; Renard, F.; Quirico, E. Removal of oxyanions from synthetic wastewater via carbonation process of calcium hydroxide: Applied and fundamental aspects. *J. Hazard. Mater.* **2009**, *166*, 788–795. [CrossRef] [PubMed]
28. Olyaie, E.; Banejad, H.; Afkhami, A.; Rahmani, A.; Khodaveisi, J. Development of a cost-effective technique to remove the arsenic contamination from aqueous solutions by calcium peroxide nanoparticles. *Separ. Purif. Technol.* **2012**, *95*, 10–15. [CrossRef]
29. Hua, C.-Y.; Lo, S.-L.; Kuan, W.-H. High concentration of arsenate removal by electrocoagulation with calcium. *Separ. Purif. Technol.* **2014**, *126*, 7–14. [CrossRef]
30. Park, Y.Y.; Tran, T.; Lee, Y.H.; Nam, Y., II; Senanayake, G.; Kim, M.J. Selective removal of arsenic (V) from a molybdate plant liquor by precipitation of magnesium arsenate. *Hydrometallurgy* **2010**, *104*, 290–297. [CrossRef]
31. Tresintsi, S.; Simeonidis, K.; Katsikini, M.; Paloura, E.C.; Bantsis, G.; Mitrakas, M. A novel approach for arsenic adsorbents regeneration using MgO. *J. Hazard. Mater.* **2014**, *265*, 217–225. [CrossRef] [PubMed]
32. Yu, X.Y.; Luo, T.; Jia, Y.; Zhang, Y.X.; Liu, J.H.; Huang, X.J. Porous hierarchically micro/nanostructured MgO: Morphology control and their excellent performance in As (III) and As (V) removal. *J. Phys. Chem. C* **2011**, *115*, 22242–22250. [CrossRef]
33. Opiso, E.M.; Sato, T.; Morimoto, K.; Asai, A.; Anraku, S.; Numako, C.; Yoneda, T. Incorporation of arsenic during the formation of Mg-bearing minerals at alkaline condition. *Miner. Eng.* **2010**, *23*, 230–237. [CrossRef]
34. Sugita, H.; Oguma, T.; Zhang, M.; Hara, J.; Kawabe, Y. Effects of silicic acid on environmental stability of spent magnesium-based arsenic adsorbents. *J. Jpn. Soc. Civ. Eng. Ser. G Environ. Res.* **2017**, *73*, 407–418. [CrossRef]
35. Sugita, H.; Oguma, T.; Hara, J.; Zhang, M.; Kawabe, Y. Effects of solution pH on spent Mg-based and Ca-based adsorbents-leaching behavior of arsenite and arsenate acids. *Jpn. Geotech. J.* **2020**, *15*, 441–453. [CrossRef]
36. Sugita, H.; Oguma, T.; Zhang, M.; Hara, J.; Takahashi, S. Environmental stability of spent magnesium-based and calcium-based arsenic adsorbents-Effects of soils. *J. Jpn. Soc. Civ. Eng. Ser. G Environ. Res.* **2016**, *72*, 437–448. [CrossRef]
37. The Chemical Society of Japan (CSJ). *Kagaku Binran (Handbook of Chemistry), Pure Chemistry II*, 4th ed.; Maruzen: Tokyo, Japan, 1993; p. 317.
38. Fujinaga, T.; Sewkido, E. *Ionic Equilibria*; Kagakudojin: Kyoto, Japan, 1967; p. 252.